

Phase Transition in Gauge Theories and Multiple Point Model

L.V.Laperashvili*

H.B.Nielsen¹⁾ **

D.A.Ryzhikh²⁾ ***

*Institute of Theoretical and Experimental Physics,
Moscow, Russia*

arXiv:hep-th/0109023v2 12 Nov 2001

¹⁾Niels Bohr Institute, Copenhagen, Denmark.

²⁾ Institute of Theoretical and Experimental Physics, Moscow, Russia.

***E-mail:** laper@heron.itep.ru

****E-mail:** hbech@alf.nbi.dk

*****E-mail:** ryzhikh@heron.itep.ru

In the present paper the phase transition in the regularized $U(1)$ gauge theory is investigated using the dual Abelian Higgs model of scalar monopoles. The corresponding renormalization group improved effective potential, analogous to the Coleman–Weinberg’s one, was considered in the two-loop approximation for β functions, and the phase transition (critical) dual and non-dual couplings were calculated in the $U(1)$ gauge theory. It was shown that the critical value of the renormalized electric fine structure constant $\alpha_{\text{crit}} \approx 0.208$ obtained in this paper coincides with the lattice result for compact QED: $\alpha_{\text{crit}}^{\text{lat}} \approx 0.20 \pm 0.015$. This result and the behavior of α in the vicinity of the phase transition point were compared with the Multiple Point Model prediction for the values of α near the Planck scale. Such a comparison is very encouraging for the Multiple Point Model assuming the existence of the multiple critical point at the Planck scale.

1. Introduction

The philosophy of the Multiple Point Model (MPM) suggested in [1] and developed in [2–4] leads to the necessity to investigate the phase transition in different gauge theories. According to MPM, there is a special point – the Multiple Critical Point (MCP) – on the phase diagram of the fundamental regularized gauge theory G , which is a point where the vacua of all fields existing in Nature are degenerate, having the same vacuum energy density. Such a phase diagram has axes given by all coupling constants considered in theory. MPM assumes the existence of MCP at the Planck scale.

A lattice model of gauge theories is the most convenient formalism for the realization of the MPM ideas. In the simplest case we can imagine our space-time as a regular hypercubic (3+1)-lattice with the parameter a equal to the fundamental (Planck) scale: $a = \lambda_P = 1/M_{Pl}$, where

$$M_{Pl} = 1.22 \times 10^{19} \text{ GeV}. \quad (1)$$

Lattice gauge theories, first introduced by Wilson [5] for studying the problem of confinement, are described by the following simplest action:

$$S = -\frac{\beta}{N} \sum_p \text{Re}(\text{Tr } \mathcal{U}_p), \quad (2)$$

where the sum runs over all plaquettes of a hypercubic lattice and \mathcal{U}_p is the product around the plaquette p of the link variables in the N -dimensional fundamental representation of the gauge group G ; $\beta = 1/g_0^2$ is the lattice constant and g_0 is the bare coupling constant of the gauge theory considered. Monte Carlo simulations of these simple Wilson lattice theories in the four dimensions showed a (or an almost) second-order deconfining phase transition for $U(1)$ [6, 7], a crossover behavior for $SU(2)$ and $SU(3)$ [8, 9], and a first-order phase transition for $SU(N)$ with $N \geq 4$ [10]. Bhanot and Creutz [11, 12] have generalized the simple Wilson action, introducing two parameters in action:

$$S = \sum_p \left[-\frac{\beta_f}{N} \text{Re}(\text{Tr } \mathcal{U}_p) - \frac{\beta_A}{N^2 - 1} \text{Re}(\text{Tr}_A \mathcal{U}_p) \right], \quad (3)$$

where β_f , Tr and β_A , Tr_A are respectively the lattice constants and traces in the fundamental and adjoint representations of $SU(N)$ considered in this action for \mathcal{U}_p . The phase diagrams, obtained for the generalized lattice $SU(2)$ and $SU(3)$ theories (3) by Monte Carlo methods in [11, 12], showed the existence of a triple point which is a boundary point of three first-order phase transitions: the "Coulomb-like" and confining $SU(N)/Z_N$, Z_N phases meet together at this point. From the triple point emanate three phase border lines which separate the corresponding phases. The Z_N phase transition is a "discreteness"

transition, occurring when lattice plaquettes jump from the identity to nearby elements in the group. The $SU(N)/Z_N$ phase transition is due to a condensation of monopoles (a consequence of the non-trivial Π_1 of the group).

Monte Carlo simulations of the $U(1)$ gauge theory, described by the two-parameter lattice action [13,14]:

$$S = \sum_{\text{p}} [\beta^{\text{lat}} \cos \Theta_{\text{p}} + \gamma^{\text{lat}} \cos 2\Theta_{\text{p}}], \quad \text{where} \quad \mathcal{U}_{\text{p}} = e^{i\Theta_{\text{p}}}, \quad (4)$$

also indicate the existence of a triple point on the corresponding phase diagram (see Fig.1): "Coulomb-like", totally confining, and Z_2 confining phases come together at the triple point shown in Fig.1.

Monte Carlo simulations of the lattice $U(1)$ gauge theory, described by the simple Wilson action corresponding to the case $\gamma^{\text{lat}} = 0$ in Eq.(4), give us [14]:

$$\alpha_{\text{crit}}^{\text{lat}} \approx 0.20 \pm 0.015 \quad \text{and} \quad \tilde{\alpha}_{\text{crit}}^{\text{lat}} \approx 1.25 \pm 0.10, \quad (5)$$

where $\alpha = e^2/4\pi$ and $\tilde{\alpha} = g^2/4\pi$ are the electric and magnetic fine structure constants, containing the electric charge e and magnetic charge g , respectively. The lattice artifact monopoles are responsible for the confinement mechanism in lattice gauge theories what is confirmed by many numerical and theoretical investigations (see reviews [15] and papers [16]). The simplest effective dynamics describing the confinement mechanism in the pure gauge lattice $U(1)$ theory is the dual Abelian Higgs model of scalar monopoles [17].

In our previous papers [1–3] the calculations of the $U(1)$ phase transition (critical) coupling constant were connected with the existence of artifact monopoles in the lattice gauge theory and also in the Wilson loop action model [3]. Here we consider the Higgs Monopole Model (HMM) approximating the lattice artifact monopoles as fundamental pointlike particles described by the Higgs scalar field. The phase border separating the Coulomb-like and confinement phases is investigated by the method developed in MPM, where degenerate vacua are considered. The phase transition Coulomb–confinement is given by the condition when the first local minimum of the effective potential is degenerate with its second minimum. Considering the renormalization group improvement of the effective Coleman–Weinberg potential [18,19] written for the dual sector of scalar electrodynamics in the two-loop approximation, we have calculated the $U(1)$ critical values of the magnetic fine structure constant $\tilde{\alpha}_{\text{crit}} = g_{\text{crit}}^2/4\pi \approx 1.20$ and electric fine structure constant $\alpha_{\text{crit}} = \pi/g_{\text{crit}}^2 \approx 0.208$ (by the Dirac relation). These values coincide with the lattice result (5).

Investigating the phase transition in HMM we have pursued two objects. From one side, we had an aim to explain the lattice results. But we had also another aim.

According to MPM, at the Planck scale there exists a multiple critical point, which is a boundary point of the phase transitions in $U(1)$, $SU(2)$, and $SU(3)$ sectors of the fundamental regularized gauge theory G . The idea of [1] was that the corresponding critical couplings coincide with the lattice ones. Our calculations in HMM indicate that the Higgs scalar monopole fields are responsible for the phase transition Coulomb–confinement, giving the same lattice values of critical couplings. By this reason, the results of the present paper are very encouraging for the Anti-Grand Unification Theory (AGUT) [20–25], which was developed previously as a realistic alternative to SUSY GUTs. This paper is also devoted to the discussion of the problems of AGUT, which is used in conjunction with MPM.

2. The Coleman–Weinberg Effective Potential for the Higgs Monopole Model

As it was mentioned in Introduction, the dual Abelian Higgs model of scalar monopoles (shortly HMM) describes the dynamics of confinement in lattice theories. This model, first suggested in [17], considers the following Lagrangian:

$$L = -\frac{1}{4g^2}F_{\mu\nu}^2(B) + \frac{1}{2}|(\partial_\mu - iB_\mu)\Phi|^2 - U(\Phi), \quad \text{where} \quad U(\Phi) = \frac{1}{2}\mu^2|\Phi|^2 + \frac{\lambda}{4}|\Phi|^4 \quad (6)$$

is the Higgs potential of scalar monopoles with magnetic charge g , and B_μ is the dual gauge (photon) field interacting with the scalar monopole field Φ . In this model λ is the self-interaction constant of scalar fields, and the mass parameter μ^2 is negative. In Eq.(6) the complex scalar field Φ contains the Higgs (ϕ) and Goldstone (χ) boson fields:

$$\Phi = \phi + i\chi. \quad (7)$$

The effective potential in the Higgs scalar electrodynamics (HSED) was first calculated by Coleman and Weinberg [18] in the one-loop approximation. The general method of its calculation is given in the review [19]. Using this method, we can construct the effective potential for HMM. In this case the total field system of the gauge (B_μ) and magnetically charged (Φ) fields is described by the partition function which has the following form in Euclidean space:

$$Z = \int [DB][D\Phi][D\Phi^+] e^{-S}, \quad (8)$$

where the action $S = \int d^4x L(x) + S_{\text{gf}}$ contains the Lagrangian (6) written in Euclidean space and gauge fixing action S_{gf} . Let us consider now a shift

$$\Phi(x) = \Phi_b + \hat{\Phi}(x) \quad (9)$$

with Φ_b as a background field and calculate the following expression for the partition function in the one-loop approximation:

$$Z = \int [DB][D\hat{\Phi}][D\hat{\Phi}^+] \exp\{-S(B, \Phi_b) - \int d^4x [\frac{\delta S(\Phi)}{\delta \Phi(x)}|_{\Phi=\Phi_b} \hat{\Phi}(x) + \text{h.c.}]\} =$$

$$= \exp\{-F(\Phi_b, g^2, \mu^2, \lambda)\}. \quad (10)$$

Using the representation (7), we obtain the effective potential:

$$V_{\text{eff}} = F(\phi_b, g^2, \mu^2, \lambda) \quad (11)$$

given by the function F of Eq.(10) for the constant background field $\Phi_b = \phi_b = \text{const.}$ In this case the one-loop effective potential for monopoles coincides with the expression of the effective potential calculated by the authors of [18] for HSED and extended to the massive theory (see review [19]):

$$V_{\text{eff}}(\phi_b^2) = \frac{\mu^2}{2}\phi_b^2 + \frac{\lambda}{4}\phi_b^4 + \frac{1}{64\pi^2}[3g^4\phi_b^4 \log \frac{\phi_b^2}{M^2} +$$

$$(\mu^2 + 3\lambda\phi_b^2)^2 \log \frac{\mu^2 + 3\lambda\phi_b^2}{M^2} + (\mu^2 + \lambda\phi_b^2)^2 \log \frac{\mu^2 + \lambda\phi_b^2}{M^2}] + C, \quad (12)$$

where M is the cut-off scale and C is a constant not depending on ϕ_b^2 .

The effective potential (11) has several minima. Their position depends on g^2, μ^2 , and λ . If the first local minimum occurs at $\phi_b = 0$ and $V_{\text{eff}}(0) = 0$, it corresponds to the so-called symmetrical phase, which is the Coulomb-like phase in our description. Then it is easy to determine the constant C in Eq.(12):

$$C = -\frac{\mu^4}{16\pi^2} \log \frac{\mu}{M}, \quad (13)$$

and we have the effective potential for HMM described by the following expression:

$$V_{\text{eff}}(\phi_b^2) = \frac{\mu_{\text{run}}^2}{2}\phi_b^2 + \frac{\lambda_{\text{run}}}{4}\phi_b^4 + \frac{\mu^4}{64\pi^2} \log \frac{(\mu^2 + 3\lambda\phi_b^2)(\mu^2 + \lambda\phi_b^2)}{\mu^4}. \quad (14)$$

Here λ_{run} is the running self-interaction constant given by Eq.(12):

$$\lambda_{\text{run}}(\phi_b^2) = \lambda + \frac{1}{16\pi^2}[3g^4 \log \frac{\phi_b^2}{M^2} + 9\lambda^2 \log \frac{\mu^2 + 3\lambda\phi_b^2}{M^2} + \lambda^2 \log \frac{\mu^2 + \lambda\phi_b^2}{M^2}]. \quad (15)$$

The running squared mass of the Higgs scalar monopoles also follows from Eq.(12):

$$\mu_{\text{run}}^2(\phi_b^2) = \mu^2 + \frac{\lambda\mu^2}{16\pi^2}[3 \log \frac{\mu^2 + 3\lambda\phi_b^2}{M^2} + \log \frac{\mu^2 + \lambda\phi_b^2}{M^2}]. \quad (16)$$

3. Renormalization group equations in the Higgs monopole model

The renormalization group equations (RGE) for the effective potential means that the potential cannot depend on a change in the arbitrary parameter – renormalization scale M , i.e., $dV_{\text{eff}}/dM = 0$. The effects of changing it are absorbed into changes in the coupling constants, masses, and fields, giving so-called running quantities.

Considering the renormalization group (RG) improvement of the effective potential [18, 19] and choosing the evolution variable as

$$t = \log(\phi^2/M^2), \quad (17)$$

we have the following RGE for the improved $V_{\text{eff}}(\phi^2)$ with $\phi^2 \equiv \phi_b^2$ [26]:

$$(M^2 \frac{\partial}{\partial M^2} + \beta_\lambda \frac{\partial}{\partial \lambda} + \beta_g \frac{\partial}{\partial g^2} + \beta_{(\mu^2)} \mu^2 \frac{\partial}{\partial \mu^2} - \gamma \phi^2 \frac{\partial}{\partial \phi^2}) V_{\text{eff}}(\phi^2) = 0, \quad (18)$$

where γ is the anomalous dimension and $\beta_{(\mu^2)}$, β_λ , and β_g are the RG β functions for mass, scalar, and gauge couplings, respectively. RGE (18) leads to the following form of the improved effective potential [18]:

$$V_{\text{eff}} = \frac{1}{2} \mu_{\text{run}}^2(t) G^2(t) \phi^2 + \frac{1}{4} \lambda_{\text{run}}(t) G^4(t) \phi^4. \quad (19)$$

In our case:

$$G(t) = \exp\left[-\frac{1}{2} \int_0^t dt' \gamma(g_{\text{run}}(t'), \lambda_{\text{run}}(t'))\right]. \quad (20)$$

A set of ordinary differential equations (RGE) corresponds to Eq.(18):

$$\frac{d\lambda_{\text{run}}}{dt} = \beta_\lambda(g_{\text{run}}(t), \lambda_{\text{run}}(t)), \quad (21)$$

$$\frac{d\mu_{\text{run}}^2}{dt} = \mu_{\text{run}}^2(t) \beta_{(\mu^2)}(g_{\text{run}}(t), \lambda_{\text{run}}(t)), \quad (22)$$

$$\frac{dg_{\text{run}}^2}{dt} = \beta_g(g_{\text{run}}(t), \lambda_{\text{run}}(t)). \quad (23)$$

So far as the mathematical structure of HMM is equivalent to HSED, we can use all results of the scalar electrodynamics in our calculations, replacing the electric charge e and photon field A_μ by magnetic charge g and dual gauge field B_μ .

The one-loop results for β_λ , $\beta_{(\mu^2)}$, β_g , and γ are given in [18,19] for scalar field with electric charge e . Using these results, we obtain for monopoles with charge $g = g_{\text{run}}$ the following expressions in the one-loop approximation:

$$\frac{d\lambda_{\text{run}}}{dt} \approx \beta_\lambda^{(1)} = \frac{1}{16\pi^2}(3g_{\text{run}}^4 + 10\lambda_{\text{run}}^2 - 6\lambda_{\text{run}}g_{\text{run}}^2), \quad (24)$$

$$\frac{d\mu_{\text{run}}^2}{dt} \approx \beta_{(\mu^2)}^{(1)} = \frac{\mu_{\text{run}}^2}{16\pi^2}(4\lambda_{\text{run}} - 3g_{\text{run}}^2), \quad (25)$$

$$\frac{dg_{\text{run}}^2}{dt} \approx \beta_g^{(1)} = \frac{g_{\text{run}}^4}{48\pi^2}, \quad (26)$$

$$\gamma^{(1)} = -\frac{3g_{\text{run}}^2}{16\pi^2}. \quad (27)$$

The RG β functions for different renormalizable gauge theories with semisimple group have been calculated in the two-loop approximation [27–32] and even beyond [33]. But in this paper we made use of the results of [27] and [30] for calculation of β functions and anomalous dimension in the two-loop approximation, applied to the HMM with scalar monopole fields.

On the level of two-loop approximation we have for all β functions:

$$\beta = \beta^{(1)} + \beta^{(2)}, \quad (28)$$

where

$$\beta_\lambda^{(2)} = \frac{1}{(16\pi^2)^2}(-25\lambda^3 + \frac{15}{2}g^2\lambda^2 - \frac{229}{12}g^4\lambda - \frac{59}{6}g^6) \quad (29)$$

and

$$\beta_{(\mu^2)}^{(2)} = \frac{1}{(16\pi^2)^2}(\frac{31}{12}g^4 + 3\lambda^2). \quad (30)$$

The gauge coupling $\beta_g^{(2)}$ function is given by [27]:

$$\beta_g^{(2)} = \frac{g^6}{(16\pi^2)^2}. \quad (31)$$

Anomalous dimension follows from the calculations made in [30]:

$$\gamma^{(2)} = \frac{1}{(16\pi^2)^2}\frac{31}{12}g^4. \quad (32)$$

In Eqs.(28)–(32) and below, for simplicity, we have used the following notations: $\lambda \equiv \lambda_{\text{run}}$, $g \equiv g_{\text{run}}$, and $\mu \equiv \mu_{\text{run}}$.

4. The phase diagram in the Higgs monopole model

Now we want to apply the effective potential calculation as a technique for the getting phase diagram information for the condensation of monopoles in HMM. As it was mentioned in Section 2, the effective potential (19) can have several minima. Their positions depend on g^2 , μ^2 , and λ . If the first local minimum occurs at $\phi = 0$ and $V_{\text{eff}}(0) = 0$, it corresponds to the Coulomb-like phase. In the case when the effective potential has the second local minimum at $\phi = \phi_{\text{min}} \neq 0$ with $V_{\text{eff}}^{\text{min}}(\phi_{\text{min}}^2) < 0$, we have the confinement phase. The phase transition between the Coulomb-like and confinement phases is given by the condition when the first local minimum at $\phi = 0$ is degenerate with the second minimum at $\phi = \phi_0$. These degenerate minima are shown in Fig.2 by the curve 1. They correspond to the different vacua arising in this model. And the dashed curve 2 describes the appearance of two minima corresponding to the confinement phases (see details in the next Section).

The conditions of the existence of degenerate vacua are given by the following equations:

$$V_{\text{eff}}(0) = V_{\text{eff}}(\phi_0^2) = 0, \quad (33)$$

$$\frac{\partial V_{\text{eff}}}{\partial \phi} \Big|_{\phi=0} = \frac{\partial V_{\text{eff}}}{\partial \phi} \Big|_{\phi=\phi_0} = 0, \quad \text{or} \quad V'_{\text{eff}}(\phi_0^2) \equiv \frac{\partial V_{\text{eff}}}{\partial \phi^2} \Big|_{\phi=\phi_0} = 0, \quad (34)$$

and inequalities

$$\frac{\partial^2 V_{\text{eff}}}{\partial \phi^2} \Big|_{\phi=0} > 0, \quad \frac{\partial^2 V_{\text{eff}}}{\partial \phi^2} \Big|_{\phi=\phi_0} > 0. \quad (35)$$

The first equation (33) applied to Eq.(19) gives:

$$\mu_{\text{run}}^2 = -\frac{1}{2} \lambda_{\text{run}}(t_0) \phi_0^2 G^2(t_0), \quad \text{where} \quad t_0 = \log(\phi_0^2/M^2). \quad (36)$$

Calculating the first derivative of V_{eff} given by Eq.(34), we obtain the following expression:

$$V'_{\text{eff}}(\phi^2) = \frac{V_{\text{eff}}(\phi^2)}{\phi^2} \left(1 + 2 \frac{d \log G}{dt}\right) + \frac{1}{2} \frac{d \mu_{\text{run}}^2}{dt} G^2(t) + \frac{1}{4} \left(\lambda_{\text{run}}(t) + \frac{d \lambda_{\text{run}}}{dt} + 2 \lambda_{\text{run}} \frac{d \log G}{dt} \right) G^4(t) \phi^2. \quad (37)$$

From Eq.(20), we have:

$$\frac{d \log G}{dt} = -\frac{1}{2} \gamma. \quad (38)$$

It is easy to find the joint solution of equations

$$V_{\text{eff}}(\phi_0^2) = V'_{\text{eff}}(\phi_0^2) = 0. \quad (39)$$

Using RGE (21), (22) and Eqs.(36)–(38), we obtain:

$$V'_{\text{eff}}(\phi_0^2) = \frac{1}{4}(-\lambda_{\text{run}}\beta_{(\mu^2)} + \lambda_{\text{run}} + \beta_\lambda - \gamma\lambda_{\text{run}})G^4(t_0)\phi_0^2 = 0, \quad (40)$$

or

$$\beta_\lambda + \lambda_{\text{run}}(1 - \gamma - \beta_{(\mu^2)}) = 0. \quad (41)$$

Substituting in Eq.(41) the functions $\beta_\lambda^{(1)}$, $\beta_{(\mu^2)}^{(1)}$, and $\gamma^{(1)}$ given by Eqs.(24), (25), and (27), we obtain in the one-loop approximation the following equation for the phase transition border:

$$g_{\text{PT}}^4 = -2\lambda_{\text{run}}\left(\frac{8\pi^2}{3} + \lambda_{\text{run}}\right). \quad (42)$$

The curve (42) is represented on the phase diagram $(\lambda_{\text{run}}; g_{\text{run}}^2)$ of Fig.3 by the curve 1 which describes the border between the "Coulomb-like" phase with $V_{\text{eff}} \geq 0$ and the confinement one with $V_{\text{eff}}^{\text{min}} < 0$. This border corresponds to the one-loop approximation. Using Eqs.(24), (25), (27)–(30), and (32), we are able to construct the phase transition border in the two-loop approximation. Substituting these equations into Eq.(41), we obtain the following equation for the phase transition border in the two-loop approximation:

$$3y^2 - 16\pi^2 + 6x^2 + \frac{1}{16\pi^2}(28x^3 + \frac{15}{2}x^2y + \frac{97}{4}xy^2 - \frac{59}{6}y^3) = 0, \quad (43)$$

where $x = -\lambda_{\text{PT}}$ and $y = g_{\text{PT}}^2$ are the phase transition values of $-\lambda_{\text{run}}$ and g_{run}^2 . Choosing the physical branch corresponding to $g^2 \geq 0$ and $g^2 \rightarrow 0$, when $\lambda \rightarrow 0$, we have received curve 2 on the phase diagram $(\lambda_{\text{run}}; g_{\text{run}}^2)$ shown in Fig.3. This curve corresponds to the two-loop approximation and can be compared with the curve 1 of Fig.3, which describes the same phase border calculated in the one-loop approximation. It is easy to see from the comparison of curves 1 and 2 that the accuracy of the one-loop approximation is not excellent and can commit errors of order 30%.

According to the phase diagram drawn in Fig.3, the confinement phase begins at $g^2 = g_{\text{max}}^2$ and exists under the phase transition border line in the region $g^2 \leq g_{\text{max}}^2$, where e^2 is large: $e^2 \geq (2\pi/g_{\text{max}})^2$ due to the Dirac relation (see below). Therefore, we have:

$$g_{\text{crit}}^2 = g_{\text{max1}}^2 \approx 18.61 \quad - \quad \text{in the one-loop approximation,}$$

$$g_{\text{crit}}^2 = g_{\text{max2}}^2 \approx 15.11 \quad - \quad \text{in the two-loop approximation.} \quad (44)$$

Comparing these results, we obtain the accuracy of deviation between them of order 20%. The results (44) give:

$$\tilde{\alpha}_{\text{crit}} = \frac{g_{\text{crit}}^2}{4\pi} \approx 1.48, \quad - \quad \text{in the one-loop approximation,}$$

$$\tilde{\alpha}_{\text{crit}} = \frac{g_{\text{crit}}^2}{4\pi} \approx 1.20, \quad - \quad \text{in the two-loop approximation.} \quad (45)$$

Using the Dirac relation for elementary charges:

$$eg = 2\pi, \quad \text{or} \quad \alpha\tilde{\alpha} = \frac{1}{4}, \quad (46)$$

we get the following values for the critical electric fine structure constant:

$$\alpha_{\text{crit}} = \frac{1}{4\tilde{\alpha}_{\text{crit}}} \approx 0.17 \quad - \quad \text{in the one-loop approximation,}$$

$$\alpha_{\text{crit}} = \frac{1}{4\tilde{\alpha}_{\text{crit}}} \approx 0.208 \quad - \quad \text{in the two-loop approximation.} \quad (47)$$

The last result coincides with the lattice values (5) obtained for the compact QED by Monte Carlo method [14].

Writing Eq.(23) with β_g function given by Eqs.(26), (28), and (31), we have the following RGE for the monopole charge in the two-loop approximation:

$$\frac{dg_{\text{run}}^2}{dt} \approx \frac{g_{\text{run}}^4}{48\pi^2} + \frac{g_{\text{run}}^6}{(16\pi^2)^2}, \quad (48)$$

or

$$\frac{d \log \tilde{\alpha}}{dt} \approx \frac{\tilde{\alpha}}{12\pi} \left(1 + 3\frac{\tilde{\alpha}}{4\pi}\right). \quad (49)$$

The values (44) for $g_{\text{crit}}^2 = g_{\text{max}1,2}^2$ indicate that the contribution of two loops described by the second term of Eq. (48) or Eq. (49) is about 0.3 confirming a validity of the perturbation theory.

In general, we are able to estimate the validity of two-loop approximation for all β -functions calculating the corresponding ratios of two-loop contributions to one-loop contributions at the maximum of curve 2, where

$$\lambda_{\text{crit}} = \lambda_{\text{run}}^{\text{max}2} \approx -7.13 \quad \text{and} \quad g_{\text{crit}}^2 = g_{\text{max}2}^2 \approx 15.11. \quad (50)$$

We have the following result:

$$\frac{\beta_{(\mu^2)}^{(2)}}{\beta_{(\mu^2)}^{(1)}} \approx -0.0637,$$

$$\frac{\beta_{\lambda}^{(2)}}{\beta_{\lambda}^{(1)}} \approx 0.0412, \quad (51)$$

$$\frac{\beta_g^{(2)}}{\beta_g^{(1)}} \approx 0.2871.$$

Here we see that all ratios are sufficiently small, i.e., all two-loop contributions are small in comparison with one-loop contributions, confirming the validity of perturbation theory in the two-loop approximation, considered in this model. The accuracy of deviation is worse ($\sim 30\%$) for β_g function. But it is necessary to emphasize that calculating the border curves 1 and 2 of Fig.3 we have not used RGE (23) for monopole charge: β_g function is absent in Eq.(41). Therefore the calculation of g_{crit}^2 according to Eq.(43) does not depend on the approximation of β_g function. The above-mentioned β_g function appears only in the second-order derivative of V_{eff} which is related with the monopole mass m (see the next section).

Eqs.(5) and (47) give the following result:

$$\alpha_{\text{crit}}^{-1} \approx 5. \quad (52)$$

This value is important for the phase transition at the Planck scale predicted by MPM.

5. Triple point

In this section we demonstrate the existence of the triple point on the phase diagram of HMM.

Considering the second derivative of the effective potential:

$$V_{\text{eff}}''(\phi_0^2) \equiv \frac{\partial^2 V_{\text{eff}}}{\partial(\phi^2)^2}, \quad (53)$$

we can calculate it for the RG improved effective potential (19):

$$\begin{aligned} V_{\text{eff}}''(\phi^2) = & \frac{V'_{\text{eff}}(\phi^2)}{\phi^2} + \left(-\frac{1}{2}\mu_{\text{run}}^2 + \frac{1}{2}\frac{d^2\mu_{\text{run}}^2}{dt^2} + 2\frac{d\mu_{\text{run}}^2}{dt}\frac{d\log G}{dt} + \right. \\ & \left. + \mu_{\text{run}}^2\frac{d^2\log G}{dt^2} + 2\mu_{\text{run}}^2\left(\frac{d\log G}{dt}\right)^2\right)\frac{G^2}{\phi^2} + \left(\frac{1}{2}\frac{d\lambda_{\text{run}}}{dt} + \frac{1}{4}\frac{d^2\lambda_{\text{run}}}{dt^2} + 2\frac{d\lambda_{\text{run}}}{dt}\frac{d\log G}{dt} + \right. \\ & \left. + 2\lambda_{\text{run}}\frac{d\log G}{dt} + \lambda_{\text{run}}\frac{d^2\log G}{dt^2} + 4\lambda_{\text{run}}\left(\frac{d\log G}{dt}\right)^2\right)G^4(t). \end{aligned} \quad (54)$$

Let us consider now the case when this second derivative changes its sign giving a maximum of V_{eff} instead of the minimum at $\phi^2 = \phi_0^2$. Such a possibility is shown in Fig.2 by the dashed curve 2. Now the two additional minima at $\phi^2 = \phi_1^2$ and $\phi^2 = \phi_2^2$ appear in our theory. They correspond to the two different confinement phases for the confinement of electrically charged particles if they exist in the system. When these two minima are degenerate, we have the following requirements:

$$V_{\text{eff}}(\phi_1^2) = V_{\text{eff}}(\phi_2^2) < 0 \quad \text{and} \quad V'_{\text{eff}}(\phi_1^2) = V'_{\text{eff}}(\phi_2^2) = 0, \quad (55)$$

which describe the border between the confinement phases conf.1 and conf.2 presented in Fig.4. This border is given as a curve $\mathcal{3}$ at the phase diagram $(\lambda_{\text{run}}; g_{\text{run}}^4)$ drawn in Fig.4. The curve $\mathcal{3}$ meets the curve 1 at the triple point A . According to the illustration shown in Fig.2, it is obvious that this triple point A is given by the following requirements:

$$V_{\text{eff}}(\phi_0^2) = V'_{\text{eff}}(\phi_0^2) = V''_{\text{eff}}(\phi_0^2) = 0. \quad (56)$$

In contrast to the requirements:

$$V_{\text{eff}}(\phi_0^2) = V'_{\text{eff}}(\phi_0^2) = 0, \quad (57)$$

giving the curve 1 , let us consider now the joint solution of the following equations:

$$V_{\text{eff}}(\phi_0^2) = V''_{\text{eff}}(\phi_0^2) = 0. \quad (58)$$

For simplicity, we have considered the one-loop approximation. It is easy to obtain the solution of Eq.(58) in the one-loop approximation, using Eqs.(54), (36), (38), and (24)–(27):

$$\mathcal{F}(\lambda_{\text{run}}, g_{\text{run}}^2) = 0, \quad (59)$$

where

$$\begin{aligned} \mathcal{F}(\lambda_{\text{run}}, g_{\text{run}}^2) = & 5g_{\text{run}}^6 + 24\pi^2 g_{\text{run}}^4 + 12\lambda_{\text{run}} g_{\text{run}}^4 - 9\lambda_{\text{run}}^2 g_{\text{run}}^2 + \\ & + 36\lambda_{\text{run}}^3 + 80\pi^2 \lambda_{\text{run}}^2 + 64\pi^4 \lambda_{\text{run}}. \end{aligned} \quad (60)$$

The dashed curve $\mathcal{2}$ of Fig.4 represents the solution of Eq.(59) which is equivalent to Eqs.(58). The curve $\mathcal{2}$ is going very close to the maximum of the curve 1 . Assuming that the position of the triple point A coincides with this maximum, let us consider the border between the phase conf.1, having the first minimum at nonzero ϕ_1 with $V_{\text{eff}}^{\text{min}}(\phi_1^2) = c_1 < 0$, and the phase conf.2 which reveals two minima with the second minimum being the deeper one and having $V_{\text{eff}}^{\text{min}}(\phi_2^2) = c_2 < 0$. This border (described by the curve $\mathcal{3}$ of Fig.4) was calculated in the vicinity of the triple point A by means of Eqs.(55) with ϕ_1 and ϕ_2 represented as $\phi_{1,2} = \phi_0 \pm \epsilon$ with $\epsilon \ll \phi_0$. The result of such calculations gives the following expression for the curve $\mathcal{3}$:

$$g_{\text{PT},3}^4 = \frac{5}{2}(5\lambda_{\text{run}} + 8\pi^2)\lambda_{\text{run}} + 8\pi^4. \quad (61)$$

The curve $\mathcal{3}$ meets the curve 1 at the triple point A .

The piece of the curve 1 to the left of the point A describes the border between the Coulomb-like phase and phase conf.1. In the vicinity of the triple point A the second derivative $V''_{\text{eff}}(\phi_0^2)$ changes its sign leading to the existence of the maximum at $\phi^2 = \phi_0^2$,

in correspondence with the dashed curve 2 of Fig.2. By this reason, the curve 1 of Fig.4 does not describe a phase transition border from the point A to the point B when the curve 2 again intersects the curve 1 at $\lambda_{(B)} \approx -12.24$. This intersection (again giving $V_{\text{eff}}''(\phi_0^2) > 0$) occurs surprisingly quickly.

The right piece of the curve 1 to the right of the point B separates the Coulomb-like phase and the phase "conf.2". But between the points A and B the phase transition border is going slightly above the curve 1. This deviation is very small and cannot be distinguished on Fig.4.

It is necessary to note that only $V_{\text{eff}}''(\phi^2)$ contains the derivative dg_{run}^2/dt . The joint solution of equations (56) leads to the joint solution of Eqs.(42) and (59). This solution was obtained numerically and gave the following triple point values of λ_{run} and g_{run}^2 :

$$\lambda_{(A)} \approx -13.4073, \quad g_{(A)}^2 \approx 18.6070. \quad (62)$$

The solution (62) demonstrates that the triple point A exists in the very neighborhood of maximum of the curve (42). The position of this maximum is given by the following analytical expressions, together with their approximate values:

$$\lambda_{(A)} \approx -\frac{4\pi^2}{3} \approx -13.2, \quad (63)$$

$$g_{(A)}^2 = g_{\text{crit}}^2|_{\text{for } \lambda_{\text{run}}=\lambda_{(A)}} \approx \frac{4\sqrt{2}}{3}\pi^2 \approx 18.6. \quad (64)$$

Finally, we can conclude that the phase diagram shown in Fig.4 gives such a description: there exist three phases in the dual sector of the Higgs scalar electrodynamics – the Coulomb-like phase and confinement phases conf.1 and conf.2.

The border 1, which is described by the curve (42), separates the Coulomb-like phase (with $V_{\text{eff}} \geq 0$) and confinement phases (with $V_{\text{eff}}^{\text{min}}(\phi_0^2) < 0$). The curve 1 corresponds to the joint solution of the equations $V_{\text{eff}}(\phi_0^2) = V_{\text{eff}}'(\phi_0^2) = 0$.

The dashed curve 2 represents the solution of the equations $V_{\text{eff}}(\phi_0^2) = V_{\text{eff}}''(\phi_0^2) = 0$.

The phase border 3 of Fig.4 separates two confinement phases. The following requirements take place for this border:

$$\begin{aligned} V_{\text{eff}}(\phi_{1,2}^2) < 0, \quad V_{\text{eff}}(\phi_1^2) = V_{\text{eff}}(\phi_2^2), \quad V_{\text{eff}}'(\phi_1^2) = V_{\text{eff}}'(\phi_2^2) = 0, \\ V_{\text{eff}}''(\phi_1^2) > 0, \quad V_{\text{eff}}''(\phi_2^2) > 0. \end{aligned} \quad (65)$$

The triple point A is a boundary point of all three phase transitions shown in the phase diagram of Fig.4. For $g^2 < g_{(A)}^2$ the field system described by our model exists in the confinement phase, where all electric charges have to be confined.

Taking into account that monopole mass m is given by the following expression:

$$V_{\text{eff}}''(\phi_0^2) = \frac{1}{4\phi_0^2} \left. \frac{d^2 V_{\text{eff}}}{d\phi^2} \right|_{\phi=\phi_0} = \frac{m^2}{4\phi_0^2}, \quad (66)$$

we see that monopoles acquire zero mass in the vicinity of the triple point A :

$$V_{\text{eff}}''(\phi_{0A}^2) = \frac{m_{(A)}^2}{4\phi_{0A}^2} = 0. \quad (67)$$

This result is in agreement with the result of compact QED [34]: $m^2 \rightarrow 0$ in the vicinity of the critical point.

6. ”ANO-strings”, or the vortex description of the confinement phases

As it was shown in the previous Section, two regions between the curves $1, 3$ and $3, 1$, given by the phase diagram of Fig.4, correspond to the existence of the two confinement phases, different in the sense that the phase conf.1 is produced by the second minimum, but the phase conf.2 corresponds to the third minimum of the effective potential. It is obvious that in our case both phases have nonzero monopole condensate in the minima of the effective potential, when $V_{\text{eff}}^{\text{min}}(\phi_{1,2} \neq 0) < 0$. By this reason, the Abrikosov–Nielsen–Olesen (ANO) electric vortices (see [35,36]) may be created in both these phases. Only closed strings exist in the confinement phases of HMM. The properties of ANO-strings in the $U(1)$ gauge theory were investigated in [37].

7. Multiple Point Model and critical values of the $U(1)$ and $SU(N)$ fine structure constants

7.1. Anti-grand unification theory

Grand Unification Theories (GUTs) were constructed with aim to extend the Standard Model (SM). The supersymmetric extension of the SM consists of taking the SM and adding the corresponding supersymmetric partners [38]. The Minimal Supersymmetric Standard Model (MSSM) shows the possibility of the existence of the grand unification point at $\mu_{\text{GUT}} \sim 10^{16}$ GeV [39]. Unfortunately, at present time experiment does not indicate any manifestation of the supersymmetry. In this connection, the Anti-Grand Unification Theory (AGUT) was developed in [20–25] as a realistic alternative to SUSY GUTs. According to this theory, supersymmetry does not come into the existence up to the Planck energy scale (1).

The SM is based on the group:

$$SMG = SU(3)_c \times SU(2)_L \times U(1)_Y. \quad (68)$$

AGUT suggests that at the scale $\mu_G \sim \mu_{P1} = M_{P1}$ there exists the more fundamental group G containing N_{gen} copies of the Standard Model Group (SMG):

$$G = SMG_1 \times SMG_2 \times \dots \times SMG_{N_{\text{gen}}} \equiv (SMG)^{N_{\text{gen}}}, \quad (69)$$

where N_{gen} designates the number of quark and lepton generations.

If $N_{\text{gen}} = 3$ (as AGUT predicts), then the fundamental gauge group G is:

$$G = (SMG)^3 = SMG_{1\text{st gen}} \times SMG_{2\text{nd gen}} \times SMG_{3\text{rd gen}}, \quad (70)$$

or the generalized one:

$$G_f = (SMG)^3 \times U(1)_f, \quad (71)$$

which was suggested by the fitting of fermion masses of the SM (see [22]).

Recently a new generalization of AGUT was suggested in [24]:

$$G_{\text{ext}} = (SMG \times U(1)_{\text{B-L}})^3, \quad (72)$$

which takes into account the see-saw mechanism with right-handed neutrinos, also gives the reasonable fitting of the SM fermion masses and describes all neutrino experiments known today.

The group G_f contains the following gauge fields: $3 \times 8 = 24$ gluons, $3 \times 3 = 9$ W bosons, and $3 \times 1 + 1 = 4$ Abelian gauge bosons.

At first sight, this $(SMG)^3 \times U(1)_f$ group with its 37 generators seems to be just one among many possible SM gauge group extensions. However, it is not such an arbitrary choice. There are reasonable requirements (postulates) on the gauge group G (or G_f , or G_{ext}) which unambiguously specify this group. It should obey the following postulates (the first two are also valid for $SU(5)$ GUT):

1. G or G_f should only contain transformations, transforming the known 45 Weyl fermions (= 3 generations of 15 Weyl particles each) – counted as left-handed, say – into each other unitarily, so that G (or G_f) must be a subgroup of $U(45)$: $G \subseteq U(45)$.
2. No anomalies, neither gauge nor mixed. AGUT assumes that only straightforward anomaly cancellation takes place and forbids the Green–Schwarz type anomaly cancellation [40].
3. AGUT should NOT UNIFY the irreducible representations under the SM gauge group, called here SMG (see Eq.(68)).

4. G is the maximal group satisfying the above-mentioned postulates.

There are five Higgs fields in the extended AGUT with the group of symmetry G_f [22]. These fields break AGUT to the SM what means that their vacuum expectation values (VEVs) are active. The extended AGUT with the group of symmetry G_{ext} given by Eq.(72) was suggested in [24] with aim to explain the neutrino oscillations. Introducing the right-handed neutrino in the model, the authors of this theory replaced the postulate 1 and considered $U(48)$ group instead of $U(45)$, so that G_{ext} is a subgroup of $U(48)$: $G_{\text{ext}} \subseteq U(48)$. This group ends up having 7 Higgs fields (see details in [24]). Typical fit to the masses and mixing angles for the SM leptons and quarks in the framework of the G_{ext} theory has shown that, in contrast to the old extended AGUT with the group of symmetry G_f , new results are more encouraging.

7.2. AGUT-MPM prediction of the Planck scale values of the $U(1)$, $SU(2)$, and $SU(3)$ fine structure constants

As it was mentioned in Introduction, the AGUT approach is used in conjunction with MPM [1–4], which assumes the existence of the Multiple Critical Point (MCP) at the Planck scale.

The usual definition of the SM coupling constants:

$$\alpha_1 = \frac{5}{3} \frac{\alpha}{\cos^2 \theta_{\overline{MS}}}, \quad \alpha_2 = \frac{\alpha}{\sin^2 \theta_{\overline{MS}}}, \quad \alpha_3 \equiv \alpha_s = \frac{g_s^2}{4\pi}, \quad (73)$$

where α and α_s are the electromagnetic and $SU(3)$ fine structure constants, respectively, is given in the Modified minimal subtraction scheme (\overline{MS}). Here $\theta_{\overline{MS}}$ is the Weinberg weak angle in \overline{MS} scheme. Using RGE with experimentally established parameters, it is possible to extrapolate the experimental values of three inverse running constants $\alpha_i^{-1}(\mu)$ (here μ is an energy scale and $i = 1, 2, 3$ correspond to $U(1)$, $SU(2)$ and $SU(3)$ groups of the SM) from the Electroweak scale to the Planck scale. The precision of the LEP data allows to make this extrapolation with small errors (see [39]). Assuming that these RGEs for $\alpha_i^{-1}(\mu)$ contain only the contributions of the SM particles up to $\mu \approx \mu_{\text{Pl}}$ and doing the extrapolation with one Higgs doublet under the assumption of a "desert", the following results for the inverses $\alpha_{Y,2,3}^{-1}$ (here $\alpha_Y \equiv \frac{3}{5}\alpha_1$) were obtained in [1] (compare with [39]):

$$\alpha_Y^{-1}(\mu_{\text{Pl}}) \approx 55.5; \quad \alpha_2^{-1}(\mu_{\text{Pl}}) \approx 49.5; \quad \alpha_3^{-1}(\mu_{\text{Pl}}) \approx 54.0. \quad (74)$$

The extrapolation of $\alpha_{Y,2,3}^{-1}(\mu)$ up to the point $\mu = \mu_{\text{Pl}}$ is shown in Fig.5.

According to the AGUT, at some point $\mu = \mu_G < \mu_{\text{Pl}}$ (but near μ_{Pl}) the fundamental

group G (or G_f , or G_{ext}) undergoes spontaneous breakdown to the diagonal subgroup:

$$G \longrightarrow G_{\text{diag.subgr.}} = \{g, g, g | g \in SMG\}, \quad (75)$$

which is identified with the usual (low-energy) group SMG. The point $\mu_G \sim 10^{18}$ GeV also is shown in Fig.5, together with a region of G theory where the AGUT works.

The AGUT prediction of the values of $\alpha_i(\mu)$ at $\mu = \mu_{\text{Pl}}$ is based on the MPM assumption about the existence of the phase transition boundary point MCP at the Planck scale, and gives these values in terms of the corresponding critical couplings $\alpha_{i,\text{crit}}$ [1, 20, 21]:

$$\alpha_i(\mu_{\text{Pl}}) = \frac{\alpha_{i,\text{crit}}}{N_{\text{gen}}} = \frac{\alpha_{i,\text{crit}}}{3} \quad \text{for } i = 2, 3, \quad (76)$$

and

$$\alpha_1(\mu_{\text{Pl}}) = \frac{2\alpha_{1,\text{crit}}}{N_{\text{gen}}(N_{\text{gen}} + 1)} = \frac{\alpha_{1,\text{crit}}}{6} \quad \text{for } U(1). \quad (77)$$

There exists a simple explanation of the relations (76) and (77). As it was mentioned above, the group G breaks down at $\mu = \mu_G$. It should be said that at the very high energies $\mu_G \leq \mu \leq \mu_{\text{Pl}}$ (see Fig.5) each generation has its own gluons, own W 's, etc. The breaking makes only linear combination of a certain color combination of gluons which exists below $\mu = \mu_G$ and down to the low energies. We can say that the phenomenological gluon is a linear combination (with amplitude $1/\sqrt{3}$ for $N_{\text{gen}} = 3$) for each of the AGUT gluons of the same color combination. This means that coupling constant for the phenomenological gluon has a strength that is $\sqrt{3}$ times smaller, if as we effectively assume that three AGUT $SU(3)$ couplings are equal to each other. Then we have the following formula connecting the fine structure constants of G theory (e.g., AGUT) and low-energy surviving diagonal subgroup $G_{\text{diag.subgr.}} \subseteq (SMG)^3$ given by Eq.(75):

$$\alpha_{\text{diag},i}^{-1} = \alpha_{1\text{st gen},i}^{-1} + \alpha_{2\text{nd gen},i}^{-1} + \alpha_{3\text{rd gen},i}^{-1}. \quad (78)$$

Here $i = U(1)$, $SU(2)$, $SU(3)$, and $i = 3$ means that we talk about the gluon couplings. For non-Abelian theories we immediately obtain Eq.(76) from Eq.(78) at the critical point (MCP).

In contrast to non-Abelian theories, in which the gauge invariance forbids the mixed (in generations) terms in the Lagrangian of G theory, the $U(1)$ sector of AGUT contains such mixed terms:

$$\frac{1}{g^2} \sum_{p,q} F_{\mu\nu,p} F_q^{\mu\nu} = \frac{1}{g_{11}^2} F_{\mu\nu,1} F_1^{\mu\nu} + \frac{1}{g_{12}^2} F_{\mu\nu,1} F_2^{\mu\nu} + \dots + \frac{1}{g_{23}^2} F_{\mu\nu,2} F_3^{\mu\nu} + \frac{1}{g_{33}^2} F_{\mu\nu,3} F_3^{\mu\nu}, \quad (79)$$

where $p, q = 1, 2, 3$ are the indices of three generations of the AGUT group $(SMG)^3$. Eq.(79) explains the difference between the expressions (76) and (77).

It was assumed in [1] that the MCP values $\alpha_{i,crit}$ in Eqs.(76) and (77) coincide with (or are very close to) the triple point values of the effective fine structure constants given by the generalized lattice $SU(3)$, $SU(2)$, and $U(1)$ gauge theories [11–14] described by Eqs.(3) and (4). Also the authors of [1] have used an assumption that the effective α_{crit} does not change its value (at least too much) along the whole borderline β of Fig.1 for the phase transition Coulomb-confinement (see details in [1]).

7.3. Multiple Point Model and the behavior of the electric fine structure constant near the phase transition point

The authors of [11–14] were not able to obtain the lattice triple point values of $\alpha_{i,crit}$ by Monte Carlo simulations method. Only the critical value of the electric fine structure constant α was obtained in [14] in the compact QED described by the simple Wilson action corresponding to the case $\gamma^{lat} = 0$ in Eq.(4). The result of [14] for the behavior of $\alpha(\beta)$ in the vicinity of the phase transition point β_T is shown in Fig.6(a) for the Wilson and Villain lattice actions. Here $\beta \equiv \beta^{lat} = 1/e_0^2$ and e_0 is the bare electric charge. The Villain lattice action is:

$$S_V = (\beta/2) \sum_p (\Theta_p - 2\pi k)^2, \quad k \in Z. \quad (80)$$

Fig.6(b) demonstrates the comparison of the functions $\alpha(\beta)$ obtained by Monte Carlo method for the Wilson lattice action and by theoretical calculation of the same quantity. The theoretical (dashed) curve was calculated by so-called Parisi improvement formula [41]:

$$\alpha(\beta) = [4\pi\beta W_p]^{-1}. \quad (81)$$

Here $W_p = \langle \cos \Theta_p \rangle$ is a mean value of the plaquette energy. The corresponding values of W_p are taken from [13].

According to Fig.6(b):

$$\alpha_{crit,theor}^{-1} \approx 8. \quad (82)$$

This result does not coincide with the lattice and HMM result (52). The deviation of theoretical calculations from the lattice ones has the following explanation: Parisi improvement formula (81) is valid in Coulomb phase where the mass of artifact monopoles is infinitely large and the photon is massless. But in the vicinity of the phase transition (critical) point the monopole mass $m \rightarrow 0$ and the photon acquires the non-zero mass

$m_0 \neq 0$. This phenomenon leads to the "freezing" of α at the phase transition point: the effective electric fine structure constant is almost unchanged in the confinement phase and approaches its maximal value $\alpha = \alpha_{\max}$. The authors of [42] predicted $\alpha_{\max} = \frac{\pi}{12} \approx 0.26$ due to the Casimir effect (see also [3]). The analogous freezing of α_s was considered in [43] in QCD. We also see that Fig.6(a) demonstrates the tendency to the freezing of α .

Now let us consider $\alpha_Y^{-1} (\approx \alpha^{-1})$ at the point $\mu = \mu_G$ shown in Fig.5. If the point $\mu = \mu_G$ is very close to the Planck scale $\mu = \mu_{\text{Pl}}$, then according to Eqs.(74) and (77), we have:

$$\alpha_{\text{1st gen}}^{-1} \approx \alpha_{\text{2nd gen}}^{-1} \approx \alpha_{\text{3rd gen}}^{-1} \approx \frac{\alpha_Y^{-1}(\mu_G)}{6} \approx 9, \quad (83)$$

what is very close to the value (82). This means (see Fig.6(b)) that in the $U(1)$ sector of G theory we have α near the critical point, therefore we can expect the existence of MCP at the Planck scale. As a consequence of such a prediction, we have to expect the change of the evolution of $\alpha_i^{-1}(\mu)$ in the region $\mu > \mu_G$ shown in Fig.5 by dashed lines. Instead of these dashed lines, we have to see the decreasing of $\alpha_i^{-1}(\mu)$ approaching to MCP at the Planck scale, where α_{crit} is close to the value (52) obtained in the present paper. But this is an aim of our future investigations based on the idea that MCP rules over the evolution of all fine structure constants in the SM and beyond it.

8. Conclusions

In the present paper we have considered the dual Abelian Higgs model of scalar monopoles reproducing a confinement mechanism in the lattice gauge theories. Using the Coleman–Weinberg idea of the RG improvement of the effective potential [18], we have considered this potential with β -functions calculated in the two-loop approximation. The phase transition between the Coulomb-like and confinement phases has been investigated in the $U(1)$ gauge theory by the method developed in MPM where degenerate vacua are considered. The comparison of the result $\alpha_{\text{crit}} \approx 0.17$ and $\tilde{\alpha}_{\text{crit}} \approx 1.48$ obtained in the one-loop approximation with the result $\alpha_{\text{crit}} \approx 0.208$ and $\tilde{\alpha}_{\text{crit}} \approx 1.20$ obtained in the two-loop approximation demonstrates the coincidence of the critical values of electric and magnetic fine structure constants calculated in the two-loop approximation of HMM with the lattice result [14]: $\alpha_{\text{crit}}^{\text{lat}} \approx 0.20 \pm 0.015$ and $\tilde{\alpha}_{\text{crit}}^{\text{lat}} \approx 1.25 \pm 0.10$. Also comparing the one-loop and two-loop contributions to β functions, we have demonstrated the validity of perturbation theory in solution of the phase transition problem in the $U(1)$ gauge theory. In the second part of our paper we have compared the prediction of AGUT and MPM for the Planck scale values of $\alpha_i^{-1}(\mu)$ with the lattice and HMM results. Such a comparison is very encouraging for MPM.

References

- [1] D. L. Bennett and H. B. Nielsen, Int. J. Mod. Phys. A **9**, 5155 (1994); A **14**, 3313 (1999).
- [2] L. V. Laperashvili, Phys. of Atom. Nucl. **57**, 471 (1994); **59**, 162 (1996).
- [3] L. V. Laperashvili and H. B. Nielsen, Mod. Phys. Lett. A **12**, 73 (1997).
- [4] L. V. Laperashvili and H. B. Nielsen, in: *Proceedings of the International Workshop on What Comes Beyond the Standard Model, Bled, Slovenia, 29 June – 9 July 1998*; Ljubljana 1999, p.15.
- [5] K. Wilson, Phys. Rev. D **10**, 2445 (1974).
- [6] M. Creutz, I. Jacobs, C. Rebbi, Phys. Rev. D **20**, 1915 (1979).
- [7] B. Lautrup, M. Nauenberg, Phys. Lett. B **95**, 63 (1980).
- [8] M. Creutz, Phys. Rev. D **21**, 2308 (1980); Phys. Rev. Lett. **45**, 313 (1980).
- [9] B. Lautrup, M. Nauenberg, Phys. Rev. Lett. **45**, 1755 (1980).
- [10] M. Creutz, Phys. Rev. Lett. **46**, 1441 (1981).
- [11] G. Bhanot, M. Creutz, Phys. Rev. D **24**, 3212 (1981).
- [12] G. Bhanot, Phys. Lett. B **108**, 337 (1982).
- [13] G. Bhanot, Nucl. Phys. B **205**, 168 (1982); Phys. Rev. D **24**, 461 (1981); Nucl. Phys. B **378**, 633 (1992).
- [14] J. Jersak, T. Neuhaus and P. M. Zerwas, Phys. Lett. B **133**, 103 (1983); Nucl. Phys. B **251**, 299 (1985).
- [15] T. Suzuki, Nucl. Phys. B Proc. Suppl. **30**, 176 (1993); R. W. Haymaker, Phys. Rep. **315**, 153 (1999).
- [16] M. N. Chernodub, M. I. Polikarpov, in *Confinement, Duality and Non-perturbative Aspects of QCD*, p.387, Ed. by Pierre van Baal, Plenum Press, 1998; hep-th/9710205; M. N. Chernodub, F. V. Gubarev, M. I. Polikarpov, A. I. Veselov, Prog. Theor. Phys. Suppl. **131**, 309 (1998); hep-lat/9802036; M. N. Chernodub, F. V. Gubarev, M. I. Polikarpov, V. I. Zakharov, hep-th/0007135.
- [17] T. Suzuki, Progr. Theor. Phys. **80**, 929 (1988); S. Maedan, T. Suzuki, Progr. Theor. Phys. **81**, 229 (1989).

- [18] S. Coleman and E. Weinberg, Phys. Rev. D **7**, 1888 (1973); S. Coleman, in *Laws of Hadronic Matter*, edited by A. Zichichi, Academic Press, New York, 1975.
- [19] M. Sher, Phys. Rep. **179**, 274 (1989).
- [20] H. B. Nielsen, in: *Proceedings of the XYII Scottish University Summer School in Physics*, St. Andrews, 1976, p.528; D. L. Bennett, H. B. Nielsen, I. Picek, Phys. Lett. B **208**, 275 (1988); H. B. Nielsen, N. Brene, Phys. Lett. B **233**, 399 (1989).
- [21] C. D. Froggatt, H. B. Nielsen, *Origin of Symmetries* (Singapore, World Scientific, 1991).
- [22] C. D. Froggatt, G. Lowe, H. B. Nielsen, Phys. Lett. B **311**, 163 (1993); Nucl. Phys. B **414**, 579 (1994); B **420**, 3 (1994); C. D. Froggatt, H. B. Nielsen, D. J. Smith, Phys. Lett. B **385**, 150 (1996); C. D. Froggatt, M. Gibson, H. B. Nielsen, D. J. Smith, Int. J. Mod. Phys. A **13**, 5037 (1998).
- [23] C. D. Froggatt, L. V. Laperashvili, H. B. Nielsen, *SUSY98, Oxford, 10–17 July 1998*; hepnts1.rl.ac.uk/susy98/.
- [24] H. B. Nielsen, Y. Takanishi, Nucl. Phys. B **588**, 281 (2000); B **604**, 405 (2001); Phys. Lett. B **507**, 241 (2001); hep-ph/0011168; hep-ph/0101181; hep-ph/0101307.
- [25] L. V. Laperashvili, in: *Proceedings of the 4th International Symposium Frontiers of Fundamental Physics, Hyderabad, India, 9–13 December 2000*.
- [26] C. G. Callan, Phys. Rev. D **2**, 1541 (1970); K. Symanzik, in: *Fundamental Interactions at High Energies*, Ed. by A. Perlmutter (Gordon and Breach, New York, 1970).
- [27] D. R. T. Jones, Nucl. Phys. B **75**, 531 (1974); Phys. Rev. D **25**, 581 (1982).
- [28] M. Fischler and C. T. Hill, Nucl. Phys. B **193** 53 (1981).
- [29] I. Jack and H. Osborn, J. Phys. A **16**, 1101 (1983).
- [30] M. E. Machacek and M. T. Vaughn, Nucl. Phys. B **222**, 83 (1983); B **249**, 70 (1985).
- [31] H. Alhendi, Phys. Rev. D **37**, 3749 (1988).
- [32] H. Arason, D. J. Castano, B. Kesthelyi, *et al*, Phys. Rev. D **46**, 3945 (1992).
- [33] O. V. Tarasov, A. A. Vladimirov, A. Yu. Zharkov, Phys. Lett. B **93**, 429 (1980); S. Larin, T. Ritberg, J. Vermaseren, Phys. Lett. B **400**, 379 (1997).

- [34] J. Jersak, T. Neuhaus, H. Pfeiffer, Phys. Rev. D **60**, 054502 (1999).
- [35] A. A. Abrikosov, Sov. Phys. JETP, **32** 1442 (1957).
- [36] H. B. Nielsen, P. Olesen, Nucl. Phys. B **61**, 45 (1973).
- [37] L. V. Laperashvili and H. B. Nielsen, Int. J. Mod. Phys. A **16**, 2365 (2001).
- [38] H.P.Nilles, Phys.Rep. **110**, 1 (1984).
- [39] P. Langacker, N. Polonsky, Phys. Rev. D **47**, 4028 (1993); D **49**, 1454 (1994); D **52**, 3081 (1995).
- [40] M. B. Green, J. Schwarz, Phys. Lett. B **149**, 117 (1984).
- [41] G. Parisi, R. Petronzio, F. Rapuano, Phys. Lett. B **128**, 418 (1983); E. Marinari, M. Guagnelli, M. P. Lombardo, *et al*, *Proceedings Lattice 91, Tsukuba 1991*, p.278; Nucl. Phys. B. Proc. Suppl. **26**, 278 (1992).
- [42] M. Lüscher, K. Symanzik, P. Weisz, Nucl. Phys. B **173**, 365 (1980).
- [43] Yu. A. Simonov, Yad. Fiz. **58**, 113 (1995); A. M. Badalian, Yu. A. Simonov, Yad. Fiz. **60**, 714 (1997); A. M. Badalian, D. S. Kuzmenko, hep-ph/0104097.

Figure captions

Figure 1. The phase diagram for $U(1)$ when the two-parameter lattice action is used. This type of action makes it possible to provoke the confinement Z_2 (or Z_3) alone. The diagram shows the existence of a triple (critical) point. From this triple point emanate three phase borders: the phase border 1 separates the totally confining phase from the phase where only the discrete subgroup Z_2 is confined; the phase border 2 separates the latter phase from the totally Coulomb-like phase; and the phase border 3 separates the totally confining and totally Coulomb-like phases.

Figure 2. The effective potential V_{eff} : the curve 1 corresponds to the Coulomb–confinement phase transition; curve 2 describes the existence of two minima corresponding to the confinement phases.

Figure 3. The one-loop (curve 1) and two-loop (curve 2) approximation phase diagram in the dual Abelian Higgs model of scalar monopoles.

Figure 4. The phase diagram (λ_{run} ; $g^4 \equiv g_{\text{run}}^4$), corresponding to the Higgs monopole model in the one-loop approximation, shows the existence of a triple point A ($\lambda_{(A)} \approx -13.2$; $g_{(A)}^2 \approx 18.6$). This triple point is a boundary point of three phase transitions: the Coulomb-like phase and two confinement phases (conf.1 and conf.2) meet together at the triple point A. The dashed curve 2 shows the requirement: $V_{\text{eff}}(\phi_0^2) = V_{\text{eff}}''(\phi_0^2) = 0$. Monopole condensation leads to the confinement of the electric charges: ANO electric vortices are created in the confinement phases conf.1 and conf.2.

Figure 5. The evolution of three inverse running constants $\alpha_i^{-1}(\mu)$, where $i = 1, 2, 3$ correspond to $U(1)$, $SU(2)$, and $SU(3)$ groups of the SM. The extrapolation of their experimental values from the electroweak scale to the Planck scale was obtained by using the renormalization group equations with one Higgs doublet under the assumption of a "desert". The precision of the LEP data allows to make this extrapolation with small errors (see [39]). AGUT works in the region $\mu_G \leq \mu \leq \mu_{\text{Pl}}$.

Figure 6. (a) The renormalized electric fine structure constant plotted versus β/β_T for the Villain action (circles) and the Wilson action (crosses). The points are obtained in [14] by the Monte Carlo simulations method for the compact QED;

(b) The behavior of the effective electric fine structure constant in the vicinity of the phase

transition point obtained with the lattice Wilson action. The dashed curve corresponds to the theoretical calculations by the Parisi improvement formula [41].

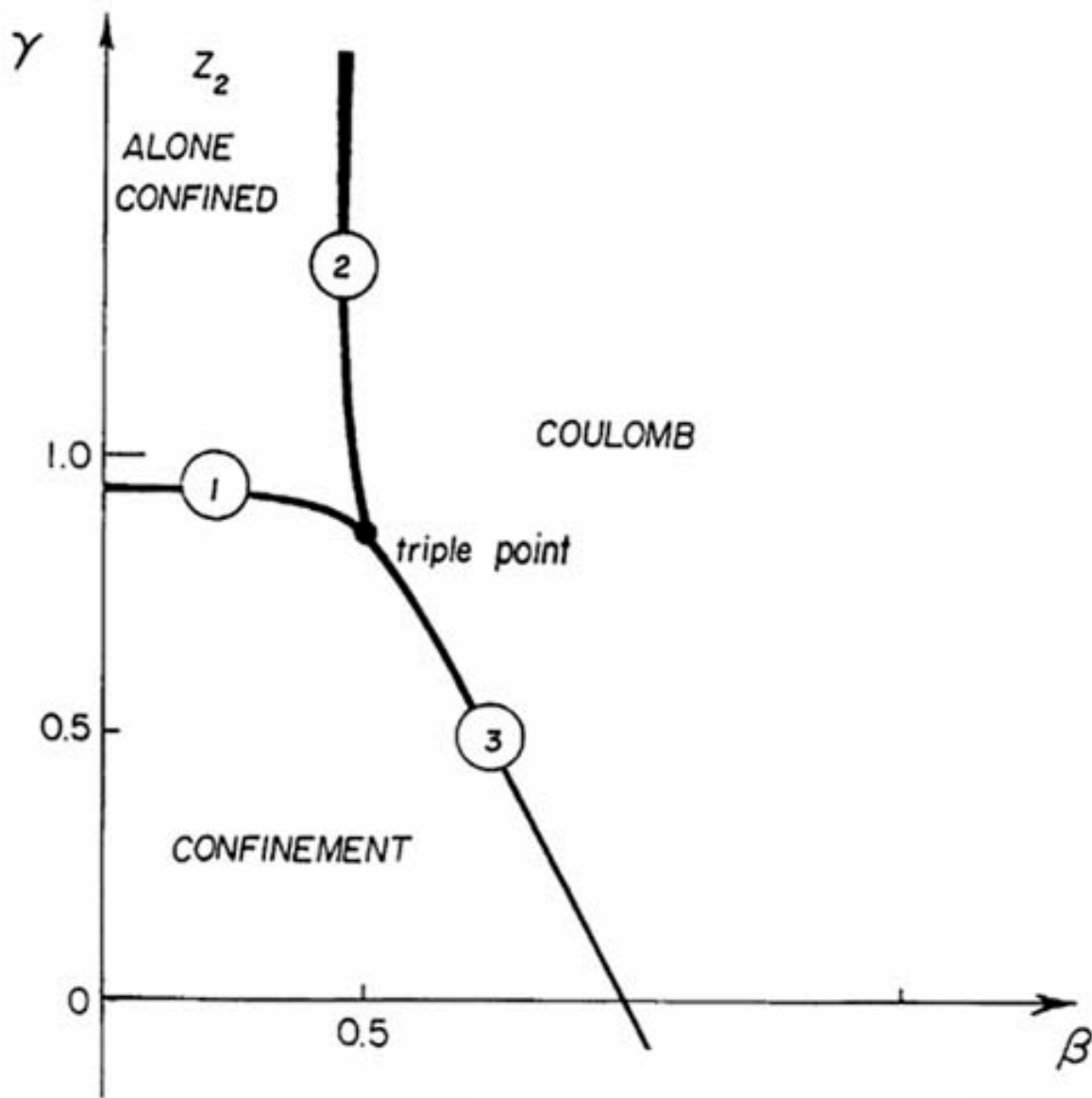


Fig.1.

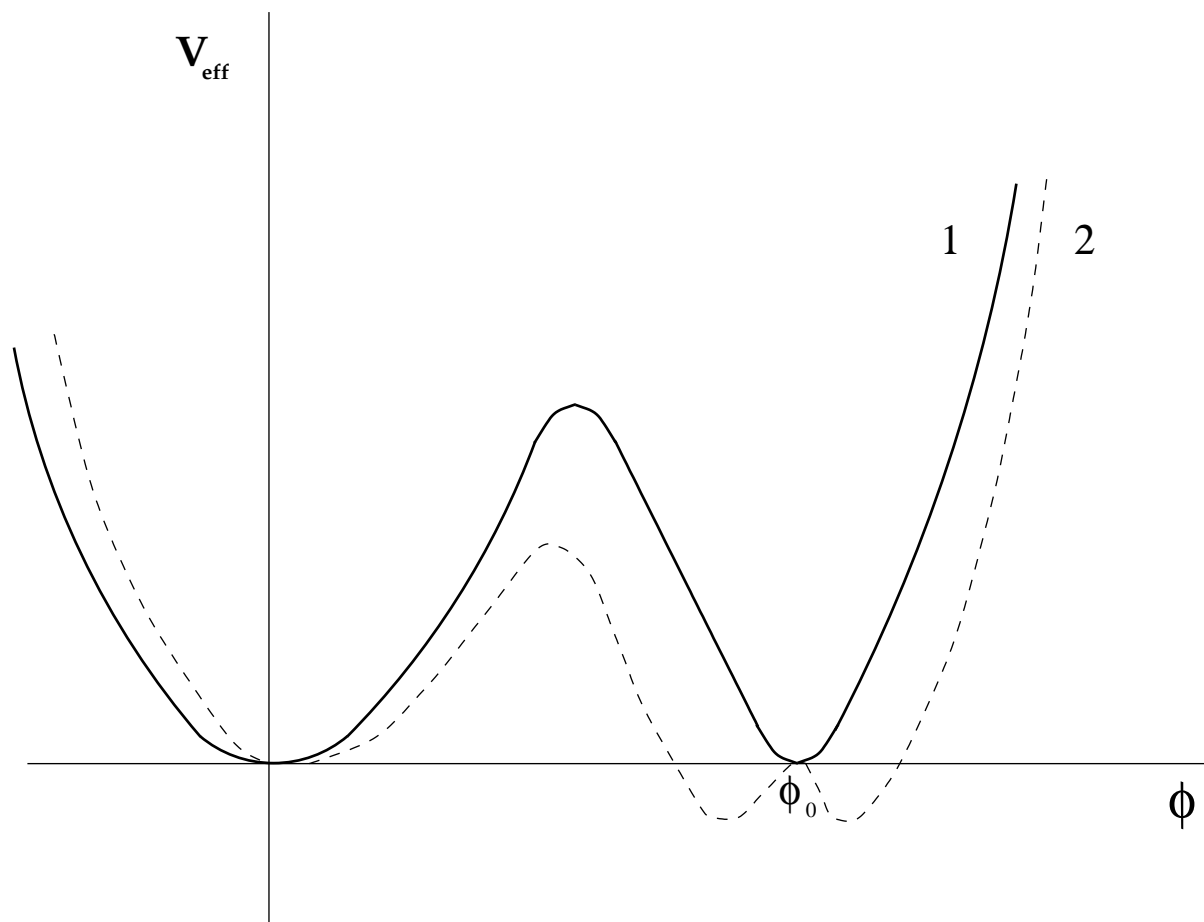


Fig.2.

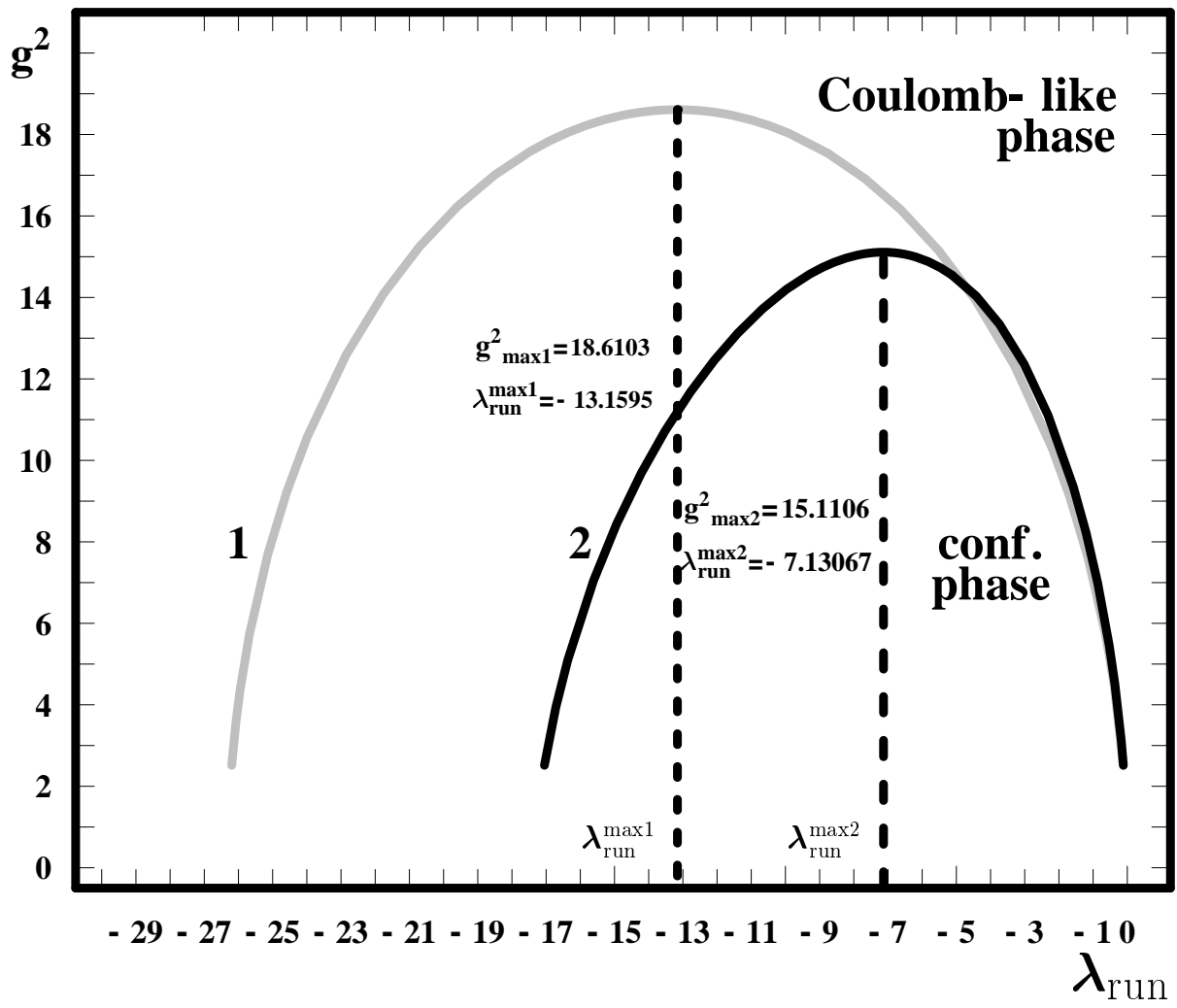


Fig.3.

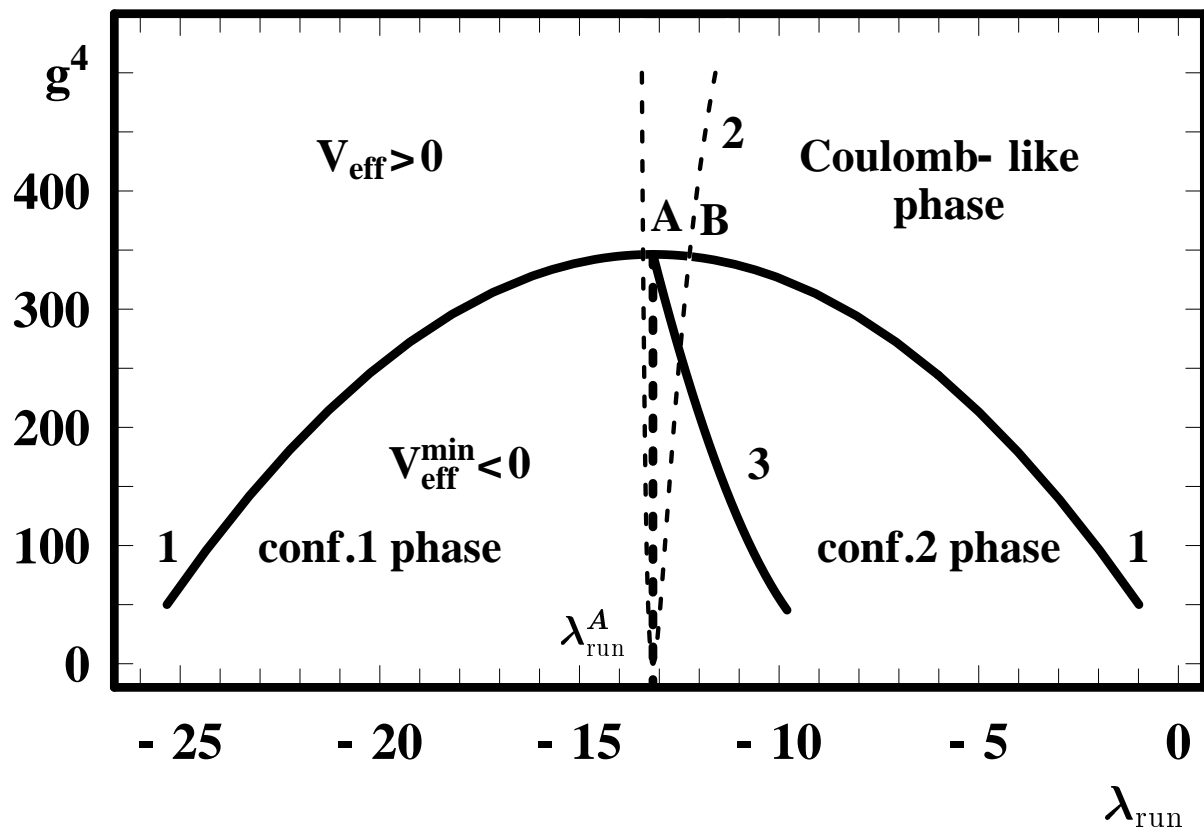


Fig.4.

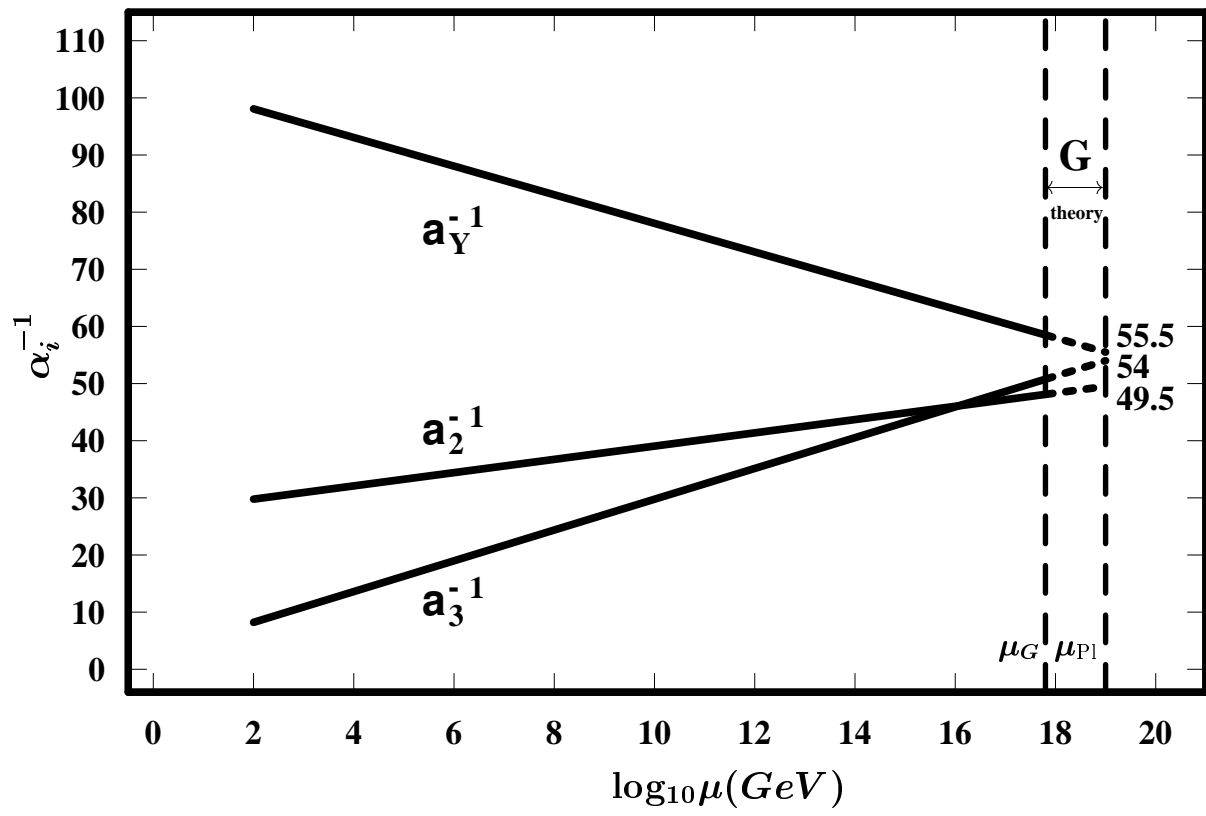


Fig.5.

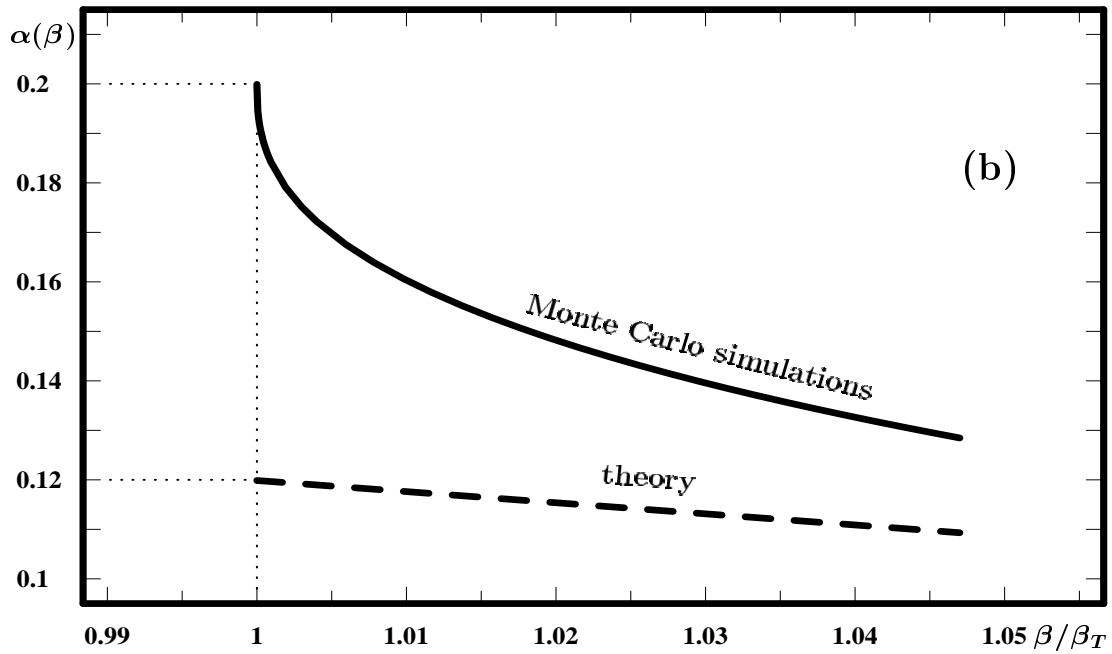
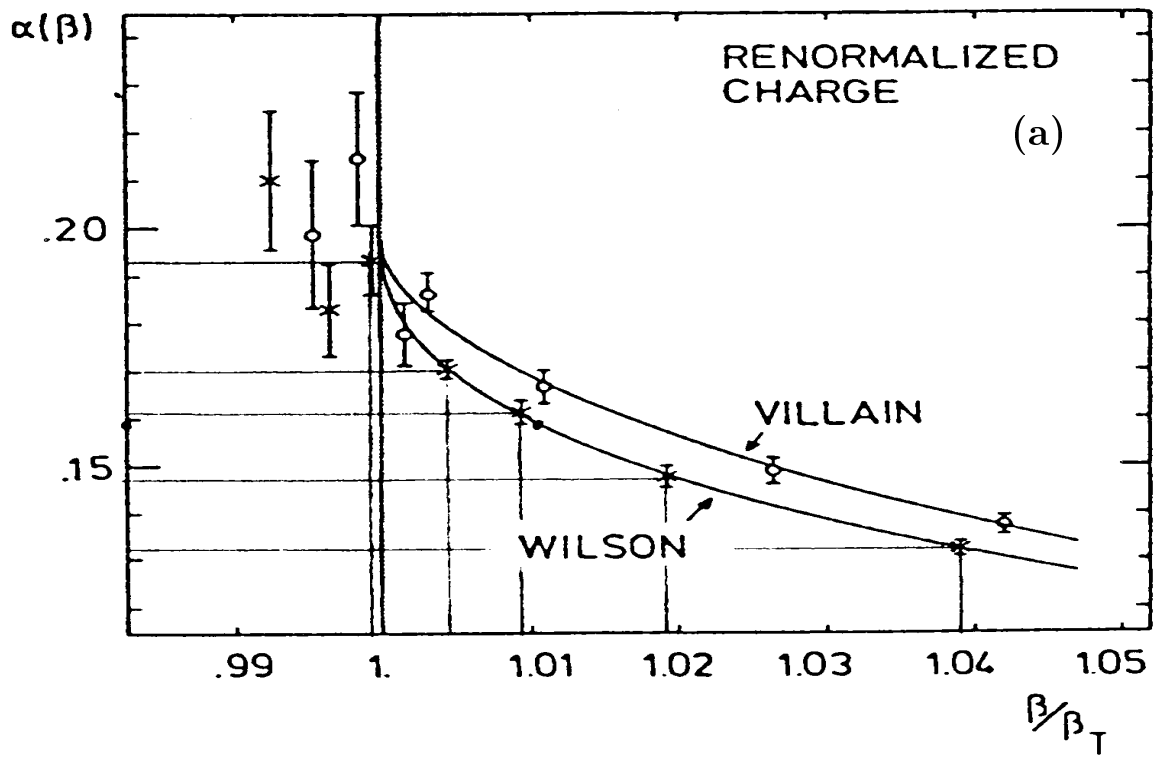


Fig.6(a,b).